

Contact Stress Analysis of Symmetrical and Asymmetrical Spur Gears Using Theoretical, Experimental and Finite Element Methods

Shivtej Ingavale¹, Prof. Dr. N. S. Dharashivkar², Prof. S. S. Mahadik³

¹M. Tech Scholar, ²Faculty of Department of Mechanical Engineering, ³Faculty of Department of Mechanical Engineering, T.K.I.E.T, Warananagar, Kolhapur, Maharashtra, India.

Abstract—Spur gears are extensively used in power transmission systems due to their simplicity, reliability, and high efficiency. The performance and service life of gears are significantly influenced by the contact stresses developed at the meshing tooth surfaces. Excessive contact stress may lead to surface fatigue, pitting, wear, and eventual failure of the gear teeth. In the present investigation, contact stress analysis of symmetrical and asymmetrical spur gears has been carried out using theoretical calculations, three-dimensional photoelastic experimentation, and finite element analysis. Theoretical stress values were determined using Hertzian contact stress theory. Experimental stress analysis was performed using stress freezing photoelasticity and fringe pattern evaluation. Finite element simulations were conducted using ANSYS Workbench to determine stress distribution under static loading conditions. Three gear configurations having pressure angles of 20°, 25°, and 30° were analyzed and compared. The obtained results indicate that contact stress decreases with an increase in drive-side pressure angle. The asymmetrical gear profile demonstrated lower contact stress and improved load-carrying capability compared to the conventional symmetrical gear. A close agreement was observed among theoretical, experimental, and finite element results, validating the effectiveness of the adopted methodology.

Keywords—Spur Gear, Contact Stress, Asymmetrical Gear, Hertz Theory, Photoelasticity, Finite Element Analysis, ANSYS.

I. INTRODUCTION

Gears are among the most important mechanical components used for transmitting power and motion between rotating shafts. Among the various types of gears, spur gears are widely employed in industrial machinery, automotive transmissions, machine tools, and power transmission systems due to their ease of manufacturing and high operational efficiency.



Fig. 1 Symmetric and Asymmetric Spur Gear

During operation, mating gear teeth are subjected to repeated contact loading. The contact between gear teeth generates compressive stresses known as Hertzian contact stresses. If these stresses exceed the allowable limits, surface deterioration such as pitting, scoring, and fatigue cracking may occur, resulting in reduced gear life and reliability.

Conventional spur gears possess symmetrical tooth profiles with identical pressure angles on both sides of the tooth. However, loading conditions on the drive side and coast side are not identical during operation. To improve load carrying capacity and reduce stress concentration, asymmetrical spur gears have been developed. These gears utilize different pressure angles on the drive and coast sides, resulting in enhanced strength characteristics and reduced contact stress.

II. LITERATURE REVIEW

Numerous researchers have investigated stress behavior in gear systems using analytical, experimental, and computational techniques.

- Faydor L. Litvin and co-workers developed asymmetric gear profiles and demonstrated their advantages in reducing stress concentration and improving load transmission characteristics.
- Alexander L.Kapelevich proposed direct design methodologies for asymmetrical gears and highlighted their increased load carrying capability.
- Bharat Gupta and researchers compared Hertzian theory with finite element analysis and observed good agreement between analytical and numerical predictions.
- Anup S. Banate and Sunil R. Patil experimentally analyzed asymmetric spur gears using photoelasticity and reported lower stress levels compared to conventional gears.

The literature indicates that asymmetrical gears exhibit superior performance under high loading conditions. However, limited work has been reported on combined theoretical, photoelastic, and finite element evaluation of contact stress.

III. OBJECTIVES

1. To determine contact stress in symmetrical and asymmetrical spur gears using theoretical analysis.
2. To evaluate contact stress experimentally using three-dimensional photoelasticity.
3. To perform finite element analysis using ANSYS software.
4. To compare theoretical, experimental, and FEA results.
5. To study the influence of pressure angle variation on contact stress distribution.

IV. THEORETICAL ANALYSIS

Hertz contact stress theory was employed for theoretical determination of contact stress between mating gear teeth.

Table I Gear Design Parameters

Parameter	Value
Module	3 mm
Power	10 kW
Pinion Speed	1440 rpm
No. of Pinion Teeth	28
No. of gear Teeth	28
Face width	30 mm
PCD of Pinion	84 mm
PCD of Gear	84 mm
Poisson's Ratio	0.3
Young's Modulus	2*105 N/mm2

According to Hertz theory, contact stress between two cylinders under compression is given by:

$$\sigma_c = \frac{2P}{\pi BL}$$

$$B = \sqrt{\frac{2P \left[\frac{1-\mu_1^2}{E_1} + \frac{1-\mu_2^2}{E_2} \right]}{\pi L \left(\frac{1}{d_1} + \frac{1}{d_2} \right)}}$$

Where:

- σ_c = maximum value of contact stress (N/mm²)
- P = force pressing the two cylinders together (N)
- B=half width of deformation (mm)
- L = axial length of cylinders (mm)
- d1, d2 = diameters of two cylinders (mm)
- E1, E2 = modulus of elasticity of two-cylinder materials (N/mm²)
- μ_1, μ_2 = Poisson's ratio of the two-cylinder materials (unitless)

Contact stress in symmetrical spur gears is given by,

$$\sigma_c^2 = \frac{1.4P_t}{bQd'_p \sin\alpha \cos\alpha \left(\frac{1}{E_1} + \frac{1}{E_2} \right)}$$

Modified Hertz equation for contact stress in asymmetric spur gear is given by,

$$\sigma_c^2 = \left[\frac{2}{\pi} \frac{F_n(1+N)E_1E_2}{NbmZ_1 \tan\alpha_c \cos\alpha_i [(1-\nu_1^2)E_2 + (1-\nu_2^2)E_1]} \right]^{0.5}$$

❖ *Case I For symmetric spur gear*

Pressure angle (α) = 20°

➤ *Torque.*

$$T = \frac{P \times 10^6 \times 60}{2\pi N}$$

$$T = 66314.56 \text{ N} - \text{mm}$$

➤ *The tangential load acting on the tooth*

$$P_t = \frac{2 \times T}{d_p}$$

$$P_t = 1578.92 \text{ N}$$

➤ The ratio factor

$$Q = \frac{2z_g}{z_g - z_p}$$

$$Q = 1$$

➤ Contact stress in symmetric spur gears

$$\sigma_c^2 = \frac{1.4P_t}{bQd'_p \sin\alpha \cos\alpha \left(\frac{1}{E_1} + \frac{1}{E_2}\right)}$$

$$\sigma_c = 522.42 \text{ N/mm}^2$$

❖ Case II For Asymmetric Spur Gear

Pressure angle (α) = 25°

Using the same torque, tangential load and ratio factor

➤ Contact stress in Asymmetric spur gears

$$\sigma_c^2 = \left[\frac{2}{\pi} \frac{F_n (1+N) E_1 E_2}{N b m Z_1 \tan \alpha_c \cos \alpha_i [(1 - \nu_1^2) E_2 + (1 - \nu_2^2) E_1]} \right]^{0.5}$$

$$\sigma_c = 447.41 \text{ N/mm}^2$$

Similar calculations were carried out for the remaining cases, and the obtained contact stress values are presented below.

Table II Theoretical Contact Stress Results

Case	Pressure Angle		Theoretical Stress (MPa)
	Coast	Drive	
I	20	20	522.42
II	20	25	447.41
III	20	30	402.09

V. EXPERIMENTAL ANALYSIS

Experimental investigation was conducted using three-dimensional photoelasticity with stress freezing technique.

A transparent photoelastic model was prepared using Araldite CY 230-1 epoxy resin and HY-951 hardener. Silicone rubber moulds were developed from actual gear specimens to accurately reproduce the tooth geometry.

5.1 The prepared mould contains a negative impression of the spur gear.



Fig. 2 Rubber Mould

5.2 The prepared mould accurately reproduces the spur gear geometry.



Fig. 3 Casting

5.3 The load was applied gradually to avoid sudden shock on the brittle photoelastic model and placed in stress freezing oven.



Fig. 4 Load Applied over Spur gear and placed in stress freezing oven.

5.4 The model is removed from the oven and thin slices are cut at critical locations.



Fig. 5 Slices

5.5 The equipment shown in below figure is Polariscope which can be used after stress freezing process take place.



Fig. 6 Polariscope

5.6 Fringes are visible under polariscope in monochromatic light



Fig. 7 Isochromatic fringe pattern at tooth root

The material fringe value of this Photoelastic material is 0.37 N/mm.

5.7 Stresses on Photoelastic Model

The fringe order for the photoelastic spur gear model was determined experimentally using a circular polariscope arrangement. During the experimental investigation, maximum fringe concentration was observed near the gear tooth contact region, indicating the presence of maximum contact stress in that area.

Specimen Calculation for Case I

The fringe order was evaluated using Tardy compensation method.

Fringe order is given by:

$$N_f = N + \frac{\theta}{180}$$

Where,

N = Fringe order of the nearest fringe with respect to the point of interest = 6

θ = Angle through which the analyzer is rotated so that the nearest fringe passes through the selected point = 96°

Substituting these values,

$$N_f = 6 + \frac{96}{180}$$

$$N_f = 6.533$$

Therefore, the fractional fringe order at the point of interest is obtained as:

$$N_f = 6.533$$

The material fringe value is: $F_\sigma = 0.37$ N/mm

The slice thickness of the model is: $h = 2$ mm

Stresses developed in the slice are given by:

$$\sigma_1 - \sigma_2 = \frac{N_f \times F_\sigma}{h}$$

Where,

σ_1, σ_2 = Maximum and Minimum Principal Stresses

N_f = Precise fringe order measured at the point of interest = 6.533

F_σ = Material fringe value = 0.37 N/mm

h = Slice thickness = 2 mm

As σ_2 is equal to zero at the boundary and σ_1 is equal to bending stress,

Therefore,

Contact stress generated in the model:

$$\sigma_m = \frac{6.533 \times 0.37}{2}$$

$$\sigma_m = 1.208 \text{ N/mm}^2$$

Hence,

Contact Stress Developed in the Photoelastic Model: $\sigma_m = 1.208 \text{ N/mm}^2$

i) Scaling Model to Prototype

The stresses were scaled from the model to the prototype using the following relation:

$$\sigma_p = \sigma_m \times \left(\frac{T_p}{T_m} \times \frac{h_m}{h_p} \times \frac{L_m}{L_p} \right) \dots\dots\dots \text{Eqn. No. 5.3}$$

T_p = the torque acting on the prototype.

T_m = the torque applied to the model.

σ_p = stress developed in the prototype.

σ_m = stress developed in the model.

As model and prototype have same dimensions.

$$L_m = L_p \text{ and } h_m = h_p$$

Therefore, the equation reduces to:

$$\sigma_p = \sigma_b \times \left(\frac{T_p}{T_m} \right)$$

We have,

$$\text{Torque on Prototype } (T_p) = 66314.56 \text{ N-mm}$$

$$\text{Torque on Model } (T_m) = 1.5 \times 9.81 \times 85$$

$$T_m = 157.63 \text{ N-mm}$$

Substituting values,

$$\sigma_p = 1.208 \times \left(\frac{6631.56}{157.63} \right)$$

$$\sigma_p = 508.64 \text{ N/mm}^2$$

Therefore,

Contact stress at root of spur gear tooth:

$$\sigma_p = 508.64 \text{ N/mm}^2$$

The experimentally obtained prototype stress was approximately 508.64 MPa.

The same experimental procedure was repeated for all gear configurations, and the corresponding contact stress values were determined.

Table III Experimental Contact Stress Results

Case	Pressure Angle		Experimental Stress (MPa)
	Coast	Drive	
I	20	20	508.64
II	20	25	435.26
III	20	30	391.84

VI. FINITE ELEMENT ANALYSIS

Finite element simulations were carried out using ANSYS Workbench.

The gear geometry was developed in SOLIDWORKS and imported into ANSYS for analysis. Structural steel was selected as the material for simulation.

Table IV Material Properties

Property	Value
Material	Structural Steel
Young's Modulus	200 GPa
Poisson's Ratio	0.3
Density	7850 kg/m ³

FEA Procedure

1. CAD model of symmetric and asymmetric spur gears was developed in SOLIDWORKS.
2. The CAD geometry was imported into ANSYS Workbench for finite element analysis.
3. Tetrahedral mesh was generated to discretize the gear model.
4. Material properties and boundary conditions were assigned.
5. Tangential load was applied on the gear tooth surface.
6. Static structural analysis was performed to determine stress and deformation.
7. Results were post-processed and compared for symmetric and asymmetric gear configurations.

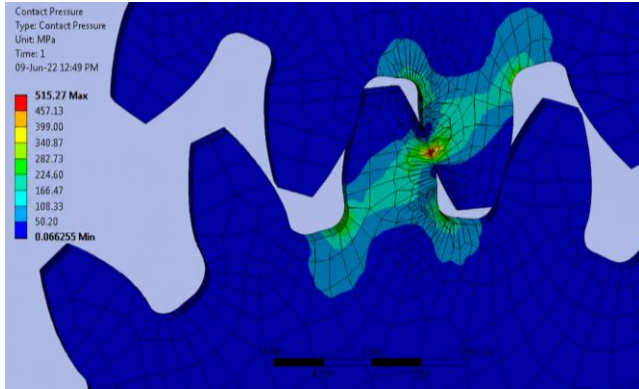


Fig. 8 Case I Stress result over Symmetric Spur Teeth

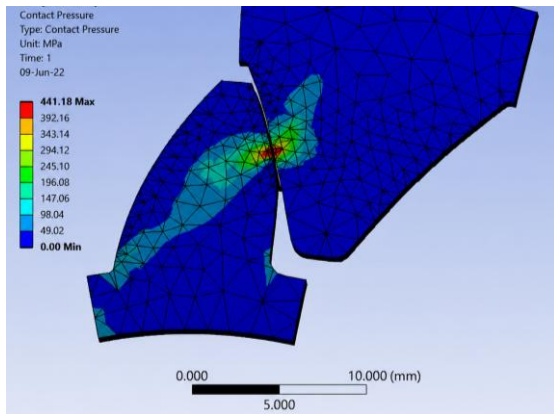


Fig. 9 Case II Stress result over Asymmetric Spur Teeth

The same procedure was repeated for the remaining cases, and the corresponding results were obtained.

Table V Finite Element Analysis Results

Case	Pressure Angle		FEA Stress (MPa)
	Coast	Drive	
I	20	20	515.27
II	20	25	441.18
III	20	30	396.52

VII. RESULTS AND DISCUSSION

Table VI Contact Stress Comparison Table

Case	Pressure Angle		Theoretical Stress (MPa)	Experimental Stress (MPa)	FEA Stress (MPa)
	Coast	Drive			
I	20	20	522.42	508.64	515.27
II	20	25	447.41	435.26	441.18
III	20	30	402.09	391.84	396.52

The results indicate a consistent reduction in contact stress with increasing drive-side pressure angle.

The asymmetrical gear configuration demonstrated improved load carrying capability due to more favorable stress distribution. The finite element predictions closely matched the experimentally obtained values, confirming the reliability of numerical simulation techniques.

VIII. CONCLUSION

1. Contact stress decreases with increasing drive-side pressure angle.
2. Asymmetrical spur gears exhibit lower stress concentration than symmetrical spur gear.
3. Finite element analysis provides accurate stress prediction.
4. Experimental photoelasticity successfully validates numerical results.
5. Maximum stress occurs near the pitch point region.
6. Asymmetrical spur gears are better suited for high-load transmission applications.

IX. FUTURE SCOPE

1. Dynamic and fatigue analysis can be performed under varying operating conditions.
2. Fatigue analysis may be performed to investigate the effect of cyclic loading on gear life and failure behavior.
3. Wear analysis can be conducted to study surface degradation and gear tooth life under prolonged operating conditions.
4. Thermal analysis may be performed to evaluate temperature distribution and thermal stresses developed during gear operation.

REFERENCES

- [1] Faydor L. Litvin, J. Matthew Hawkins, Alfonso Fuentes and Robert F. Handschuh, paper on “Design Generation and Tooth Contact Analysis of Asymmetric Face Gear Drive with Modified Geometry”, NASA/TM-2001-210614, pp. 1–30, January 2001.
- [2] Anup S. Banate and Sunil R. Patil, paper on “Contact Stress Analysis of Asymmetric Spur Gear Using Photoelasticity Experiment”, International Research Journal of Engineering and Technology (IRJET), Vol. 07, Issue 04, pp. 6599–6603, April 2020.
- [3] Mohammad Qasim Abdullah and Adnan Naama Abood, paper on “Experimental and Numerical Studies on the Contact Stresses in Asymmetric Spur Gears”, 1st International Conference on Recent Trends of Engineering Sciences and Sustainability, pp. 1–8, May 2017.
- [4] Benny Thomas, K. Sankaranarayanan, S. Ramachandra and S. P. Suresh Kumar, paper on “Selection of Pressure Angle Based on Dynamic Effects in Asymmetric Spur Gear with Fixed Normal Contact Ratio”, Defence Science Journal, Vol. 69, No. 3, pp. 303–310, May 2019.



International Journal of Recent Development in Engineering and Technology
Website: www.ijrdet.com (ISSN 2347-6435 (Online) Volume 15, Issue 06, June 2026)

- [5] Faydor L. Litvin, Qiming Lian and Alexander L. Kapelevich, paper on “Asymmetric Modified Spur Gear Drives: Reduction of Noise, Localization of Contact, Simulation of Meshing and Stress Analysis”, *Computer Methods in Applied Mechanics and Engineering*, Vol. 188, pp. 363–390, 2000.
- [6] Bharat Gupta, Abhishek Choubey and Gautam V. Varde, paper on “Contact Stress Analysis of Spur Gear”, *International Journal of Engineering Research and Technology (IJERT)*, Vol. 1, Issue 4, June 2012.
- [7] G. Mallesh, V. B. Math, Venkatesh, Shankarmurthy H. J., Shiva Prasad P. and Aravinda K., paper on “Parametric Analysis of Asymmetric Spur Gear Tooth”, 14th National Conference on Machines and Mechanisms, December 17–18, 2009.
- [8] Prashant Patil, Narayan Dharashiwar, Krishnakumar Joshi, Mahesh Jadhav “3D Photoelastic and Finite Element Analysis of Helical Gear” *machine design*, Vol.3 2011 No.2, ISSN 1821-1259 pp. 115-120.